Journal of Hazardous Materials 392 (2020) 122335

Contents lists available at ScienceDirect

Journal of Hazardous Materials

journal homepage: www.elsevier.com/locate/jhazmat

Stormwater green infrastructures retain high concentrations of TiO_2 engineered (nano)-particles

Mohammed Baalousha[a,*], Jingjing Wang[a], Md. Mahmudun Nabi[a], Frédéric Loosli[a], Renan Valenca[b], Sanjay K. Mohanty[b], Nabiul Afrooz[c], Elizabeth Cantando[d], Nirupam Aich[e]

[a] Center for Environmental Nanoscience and Risk, Department of Environmental Health Sciences, Arnold School of Public Health, University of South Carolina, Columbia, SC, United States
[b] Department of Civil and Environmental Engineering, University of California Los Angeles, CA, United States
[c] Southern California Coastal Water Research Project, Costa Mesa, CA, United States
[d] Virginia Tech National Center for Earth and Environmental Nanotechnology (NanoEarth), 1991 Kraft Dr., Blacksburg, VA 24061, United States
[e] Department of Civil, Structural and Environmental Engineering, University at Buffalo, Buffalo, NY 14260, United States

GRAPHICAL ABSTRACT

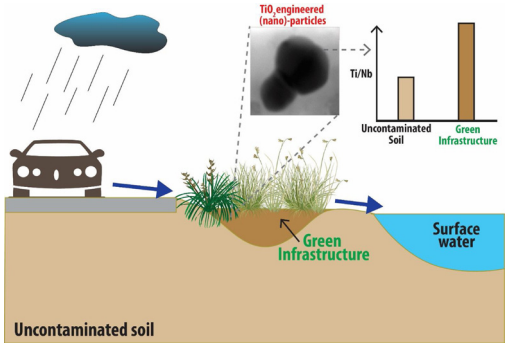

ARTICLE INFO

Editor: D. Aga

Keywords:
Titanium dioxide
Stormwater green infrastructures
Engineered (nano)-particles
Detection
Quantification
Elemental ratios
Niobium

ABSTRACT

Stormwater conveys natural and engineered (nano)-particles, like any other pollutants, from urban areas to water resources. Thus, the use of stormwater green infrastructures (SGI), which infiltrate and treat stormwater, can potentially limit the spread of engineered (nano)-particles in the environment. However, the concentration of engineered (nano)-particles in soil or biofilter media used in SGI has not been measured due to difficulties in distinguishing natural *vs.* engineered (nano)-particles. This study reports, for the first time, the concentration and size distribution of TiO_2 engineered (nano)-particles in soils collected from SGI. The concentrations of TiO_2 engineered (nano)-particles were determined by mass balance calculations based on shifts in elemental concentration ratios, *i.e.,* Ti to Nb, Ti to Ta, and Ti to Al in SGI soils relative to natural background elemental ratios. The concentrations of TiO_2 engineered (nano)-particles in SGI soils varied between 550 ± 13 and 1800 ± 200 mg kg^{-1}. A small fraction of TiO_2 engineered (nano)-particles could be extracted by ultrapure water (UPW) and $Na_4P_2O_7$; however, the concentration of TiO_2 engineered (nano)-particles was higher in the $Na_4P_2O_7$-extracted suspensions than in UPW-extracted suspensions. The concentration of TiO_2 in the nanosize range increased with the increase in extractant ($Na_4P_2O_7$) volume to soil mass ratio due to the increased disaggregation of soil heteroaggregates. The size distribution of TiO_2 engineered (nano)-particles in the < 450 nm $Na_4P_2O_7$-extracted suspension from one of the SGI soils was determined by asymmetrical flow-field flow fractionation coupled to

* Corresponding author.
E-mail address: mbaalous@mailbox.sc.edu (M. Baalousha).

https://doi.org/10.1016/j.jhazmat.2020.122335
Received 1 December 2019; Received in revised form 13 February 2020; Accepted 15 February 2020
Available online 17 February 2020

inductively coupled plasma-mass spectrometer, and was found to vary in the range of 25 − 200 nm with a modal size of 50 nm. These results demonstrated that the increase in the Ti to natural tracers (*e.g.,* Nb, Ta, and Al) elemental ratios in the SGI soil relative to bulk soil can be used to estimate the concentration of TiO_2 engineered (nano)-particles in SGI.

1. Introduction

Urbanization increases the release of contaminants, including engineered and anthropogenic (nano)-particles, from the urban developments through runoff into receiving water bodies (Gnecco et al., 2005; Kondo et al., 2016; Wang et al., 2019), resulting in surface water quality impairment (Ahiablame et al., 2012; He et al., 2001). To mitigate surface water contamination, stormwater green infrastructures (SGI) - an approach to water management that protects, restores, or mimics the natural water cycle - such as retention ponds, biofilters, bioinfiltration systems, and bioswales are incorporated into city development plan to capture and treat contaminants in urban runoff (Birch et al., 2005). SGI have been shown to remove particulate contaminants by settling, deposition, filtration, and adsorption and to remove dissolved pollutants by filtration, adsorption, and degradation (Grebel et al., 2013; Li et al., 2019). However, the occurrence and concentrations of engineered (nano)-particles in SGI has not been evaluated, despite the widespread use of engineered (nano)-particles in the urban environment (Baalousha et al., 2016).

TiO_2 is widely used in the urban environment in paint as a pigment (*e.g.,* 100 − 300 nm) and in self-cleaning surfaces as photocatalyst nanoparticles (*e.g.,* 1 − 100 nm) (Baalousha et al., 2016). The United States paint demand is estimated at 5.3 billion liters $year^{-1}$ in 2019, a third of which (*e.g.,* 1.77 billion liters) is used for exterior paint (Coatingsworld, 2019). The mass of road marking in the United States is estimated at 350,000 metric tons $year^{-1}$ in 2018 and is forecast to reach 450,000 metric tons $year^{-1}$ in 2025 (Grand View Research, 2018). White road marking contains at least 10 % wt TiO_2 pigments (ASTM, 2015), corresponding to at least 35,000 metric tons TiO_2 pigment $year^{-1}$ in 2018 and to at least 45,000 metric tons TiO_2 pigment $year^{-1}$ in 2025. TiO_2 engineered (nano)-particles from these sources (*e.g.,* paint and road marking) are expected to be released into the environment by wear and tear (Gohler et al., 2010; Golanski et al., 2012; Shandilya et al., 2014a, 2015; Shandilya et al., 2014b), which in turn deposit on surfaces *via* dry and wet deposition (Lee et al., 2016). Subsequently, wet and dry-weather runoff washes these particles from surfaces in the urban environment and carries them to surface waters (Wang et al., 2019), unless they are intercepted by SGI. However, there is currently no data on the occurrence and concentrations of engineered (nano)-particles, such as TiO_2, in SGI due to the difficulties in quantifying engineered (nano)-particle in natural soils. Quantifying the concentrations of engineered (nano)-particles, including TiO_2, in soils is challenging because of the similarity in the elemental composition of engineered (nano)-particles and those of natural nanoparticles and larger sized engineered particles (*e.g.,* pigments) and the tendency of natural and engineered (nano)-particles to form heteroaggregates in the natural environment (Praetorius et al., 2017; Wang et al., 2015). Nonetheless, few studies investigated the detection and quantification of engineered particles (*e.g.,* CeO_2, Ag, and Cu) in soils spiked with engineered (nano)-particles (Mahdi et al., 2017; Navratilova et al., 2015; Praetorius et al., 2017).

The proposed approaches to measure engineered (nano)-particles in environmental samples rely on tracing their physiochemical properties (*e.g.* elemental composition (Tong et al., 2015), elemental ratios (Gondikas et al., 2014; von der Kammer et al., 2012), size and morphology (Luo et al., 2011), fluorescence (Part et al., 2015)), which are expected to display subtle differences compared to those of natural homologous particles. For instance, naturally occurring TiO_2 particles contain other elements such as Al, Fe, Ce, Si, La, Zr, Nb, Pb, Ba, Th, Ta, W and U, whereas TiO_2 engineered particles are relatively pure (Gondikas et al., 2014). Natural TiO_2 minerals have been shown to be the dominant carrier phase (> 90-95 % of whole rock content) for Nb (José and Wyllie, 1983; Nakashima and Imaoka, 1998). This principle (*i.e.,* elemental ratios) has been recently implemented to quantify the concentration of TiO_2 engineered (nano)-particles in surface waters impacted by sewage spills (Loosli et al., 2019a) and urban runoff (Wang et al., 2019). These findings were further supported by morphological differences, observed using transmission electron microscopy (TEM), between engineered particles (typically facetted) and natural particles (typically irregular) (Loosli et al., 2019; Wang et al., 2019).

Spectroscopic approaches, such as inductively coupled plasma-mass spectrometry (ICP-MS), and energy dispersive spectroscopy (EDS) coupled to TEM, are the most widely used methods to analyze metal and metal oxide engineered nanoparticles (ENPs in complex samples due to their chemical specificity (von der Kammer et al., 2012). Single element- single particle inductively coupled plasma-mass spectroscopy (SE-SP-ICP-MS) has been used to detect and measure the size of Ag ENPs (Huynh et al., 2016; Mahdi et al., 2017). More recently, multi element-SP-ICP-MS has been applied to differentiate natural and engineered particles (*e.g.,* CeO_2 (Praetorius et al., 2017) and TiO_2 (Gondikas et al., 2018; Loosli et al., 2019a)). Additionally, asymmetrical flow-field flow fractionation (AF4-ICP-MS) has been implemented to detect, quantify, and size Ag ENPs in soils (Huynh et al., 2016). These methods require particle extraction prior to analysis to facilitate engineered (nano)-particles characterization. Engineered (nano)-particles tend to form heteroaggregates with natural particles and natural organic matter in soils (Buffle et al., 1998). Heteroaggregation is one of the key challenges that hampers engineered (nano)-particle characterization (Loosli et al., 2014, 2015). Thus, nanoparticle extraction from soil microaggregates is a key process to simplify their characterization by reducing sample polydispersity and to improve the understanding of engineered (nano)-particles physicochemical properties such as size distribution, elemental composition and ratios, and morphology (Montano et al., 2014; Regelink et al., 2013). We demonstrated recently that $Na_4P_2O_7$ is an efficient extractant to disaggregate natural nanoparticle aggregates from soils (Loosli et al., 2019b).

This study aims to (1) quantify the concentration of TiO_2 engineered (nano)-particles in SGI, (2) evaluate the effect of extraction parameters (*e.g.,* extractant composition and soil mass to extractant volume ratio) on the extraction of natural and engineered TiO_2 particles, and (3) characterize physicochemical properties of the extracted particle suspensions such as size distribution, morphology, elemental composition and ratios by AF4-ICP-MS and TEM. Identifying and quantifying the concentrations of engineered (nano)-particles in SGI is critical in assessing the potential of the stormwater treatment systems to reduce the environmental exposures of engineered (nano)-particles and the impact of engineered (nano)-particles on the ability of stormwater systems to serve other ecosystem functions.

2. Material and methods

2.1. Sampling sites

Multiple SGI sites were inspected and sites with clearly defined inlet structures from Orange County (OC1, OC2, OC3, and OC4) and Los Angeles (LA2, LA3, LA4, and LA5; Table 1, Fig. 1), California, United States were selected for soil sampling. OC1 and OC2 sites are biofilter and bioswale SGI, respectively, which are located in urban commercial

Table 1
Storm water green infrastructures (SGI) sites selected for sampling of topsoil at the inlet.

Sampling label	Site Name	SGI Type	Latitude	Longitude	Primary Land Use	Runoff Source	Age (years)	Distance from major traffic sources (m)	Collection area (m^2)
OC1	Collins Yard	Biofilter	33.802524	−117.874209	Urban/Industrial	Parking Lot	11	365	10,000
OC2	Walgreens Bioswale	Bioswale	33.787304	−117.837294	Commercial	Parking Lot	11	460	7000
OC3	Orange County Public Works Campus	Bioretention	33.826111	−117.851857	Urban	Parking Lot	3	1750	20,000 (approx.)
OC4	San Joaquin Marsh	Retention Pond	33.6613889	−117.84166667	Urban	Dry and wet weather runoff	17	450	–
LA1	Marina Del Ray Parking Lot 5	Not aa SGI, approximately 10 m from LA2	33.982515	−118.442323	Urban	Parking Lot	N/A	60	N/A
LA2	Marina Del Ray Parking Lot 5	Biofilter followed by Modular Wetland	33.982515	−118.442323	Urban	Parking Lot	5	60	2,000
LA3	Marina Del Ray Parking Lot 7	Biofilter followed by Modular Wetland	33.985125	−118.450851	Urban	Parking Lot	5	300	900
LA4	Jackson avenue near Ballona Creek	Bioswale	34.012290	−118.392070	Urban/residential	Parking lot	–	1650	10,000
LA5	North Atwater Park near LA River	Bioswale	34.1328605	−118.2730335	Urban/ industrial	Parking lot	< 5 years	150	1,200

OC: Orange County.
LA: Los Angeles.

areas. These SGI receive and infiltrate runoff from the surrounding parking lots, discharge treated runoff to Santa Ana River. OC3 site is a SGI demonstration site where a combination of different types of SGI, including bioretention, permeable pavement, and biofilters, are utilized to treat urban runoff generated from the Orange County Public Works campus. The OC3 sample was collected from a bioretention SGI. The OC4 sample was collected from the bottom of a stormwater retention basin, which is a part of a series of retention basins at San Joaquin Marsh within Irvine Water District. San Joaquin Marsh works as a natural treatment system that receives dry and wet weather runoff from San Diego Creek and protects the environmentally sensitive Upper Newport Bay. The upper 1.5 cm of soil from SGI inlet was scraped and collected in a plastic bag. For each site, approximately 250 − 350 g of soil was collected, stored, and used for laboratory analysis. All samples were collected on March 31, 2018 between 10 a.m. and 5 pm.

LA1-3 sites are located near Marina Del Rey Harbor (MDR). MDR is currently designated as an “impaired” waterbody on the 303(d) list under the United States Clean Water Act. Site LA2 is a Modular Wetlands System (MWS) linear bio-filtration treatment system that was designed and implemented to treat parking lot runoff before it discharges to the Basin. The LA1 sample was collected from a spot approximately 10 m away from the LA2 sampling location. While this spot (LA1) was not within the biofilters, the sampling spot was not protected from exposure to runoff. LA3 site is a bioretention swale that captures and treats runoff prior to the stormwater discharge onto MDR basin. LA4 was collected from a bioswale located near the end of a parking lot in a residential area adjacent to Ballona Creek. Runoff generated from this residential area is channeled into the bioswale, collecting particles deposited on the residential properties. The LA4 location is approximately 1.6 km from two major freeways (Golden State Freeway, dual carriageway, 5 lane each) in Los Angeles. On the other hand, the LA5 sample point is located in a bioswale on the side of a parking lot located in North Atwater Park adjacent to the LA River. Because the LA5 location is within 150 m of the Golden State Freeway, airborne dust generated from the highway is expected to be deposited on the parking lot, where stormwater can convey it to the bioswale.

2.2. Particle extraction

Two types of solution were used to extract particles from soils: 1) UPW, at pH 10 (Tang et al., 2009), and 2) 10 mM tetrasodium pyrophosphate ($Na_4P_2O_7$, Analytical grade, Alfa Aesar) at pH 10 (Regelink et al., 2013. Extraction was performed by mixing 1000 mg, 100 mg, or 10 mg of freeze-dried soil with 10 mL extraction solution in a 15-mL acid-washed centrifuge tube. The mixture was first stirred in a tube rotator Multi-purpose tube rotator, Fisher Scientific at 40 rpm for 20 h to allow interaction between soil and media, followed by sonication for 1 h to break heteroaggregates and release particles. Separation of different size fractions of the extracted sample was achieved by centrifugation (Eppendorf Centrifuge 5810 R) (Fedotov et al., 2011). The centrifugation speed and settling time were calculated assuming a particle density of 2.5 $g\ cm^{-3}$. The < 1000 nm, < 450 nm, and the < 100 nm size fractions were obtained by centrifuging the extracted suspensions at 750 g for 6 min, 750 g for 30 min, and 3100 g for 130 min, respectively. The top 8 ml were decanted and stored for further analysis.

2.3. Elemental analysis

The elemental concentrations of the bulk soils and the extracted suspensions were determined by ICP-MS following acid digestion according to the protocols described in detail in the supplementary information section (SI 1) and elsewhere (Loosli et al., 2019a). Briefly, the soils from the SGI and the sediment from the retention pond were sieved using a 2 mm pore size plastic sieve (PE, 10 mesh, Zhangxing). The sieved soils and sediments were freeze dried (Labconco Freeze Dry

Fig. 1. Sampling locations near stormwater green infrastructures (SGI) distributed in urban areas in Los Angeles, California, USA.

System) at -40 °C and < 130 × 10^{-3} mbar for at least 24 h. The extracted particle suspensions (8 mL of each aqueous sample) were dried at 110 °C in digestion vessels. The freeze-dried soils and sediments and the dried particle suspension residue were digested with HF:HNO_3 (3:1) mixture (ACS grade acids distilled in the laboratory) in a custom-made digestion oven in a metal-free HEPA filtered air clean lab. The elemental concentrations of the digested samples were determined using Perkin Elmer NexION 350D ICP-MS.

2.4. Size-based elemental analysis

Size-based elemental distribution analysis was performed by coupling Wyatt Eclipse DualTec asymmetrical flow-field flow fractionation (AF4) with Perkin Elmer NexION350D. All separation experiments on AF4 used regenerated cellulose membranes (Superon) with 10 kDa molecular weight cut-off. The carrier solution used in AF4 channel with a 350 μm spacer was composed of 18 mΩ cm^{-1} UPW consisting of 0.0125 % FL-70 (Fisher Chemicals), 0.01 % NaN_3 (Fisher BioReagents), and 10 mM $NaNO_3$ (ACS grade, AMRESCO). The detector flow was set to 1.0 mL min^{-1}, while a constant cross flow of 0.5 mL min^{-1} was applied during 70 min elution time. Latex nanosphere size standards in sizes 20, 40, 80, and 150 nm (Thermo Scientific) were used to calibrate particle size *vs*. retention time under the same experimental conditions for samples.

ICP-MS was tuned using the same standard procedure described in the supplementary information section (SI 1). For ICP-MS calibration, the sample introduction tubing and the internal standard introduction tubing were connected to a Y-connector (PEEK, Analytical Sales & Services). PVC 2-stop flared pump tubing with 0.762 mm ID (Meinhard) was used as sample tubing to obtain flow rate of 1.0 mL min^{-1} to match the AF4 detector flow. Calibration was performed using the same ICP-MS standards described in the supplementary information section (SI 1), with concentration ranging from 0.1–100 μg L^{-1}. After mass concentration calibration, the AF4 outlet line was connected to the Y-connector, replacing the sample tubing. AF4 separated particles were continuously introduced into the ICP-MS with a constant 10 μg L^{-1} internal standard to monitor and correct any possible signal drift over time. Between samples, a 20-min 1% HNO_3 rinse followed by a 10-min UPW rinse was applied. AF4-ICP-MS data was collected using Chromera 4.1.0.6386 software.

2.5. Calculation of engineered Ti concentration

The concentrations of TiO_2 engineered (nano)-particles were determined by mass balance calculations based on shifts in elemental concentration ratios of Ti to Nb, Ti to Ta, and Ti to Al in SGI soils relative to the corresponding natural background elemental concentration ratio (Loosli et al., 2019; Wang et al., 2019).

$$Ti_{natural} = Tracer_{sample} \times \left(\frac{Ti}{Tracer}\right)_{background} \quad (1)$$

$$Ti_{engineered} = Ti_{sample} - Ti_{natural} \quad (2)$$

Where, Ti_{sample}, $Ti_{natural}$ and $Ti_{engineered}$ are the total, natural, and engineered Ti concentration in the sample, $Tracer_{sample}$ is the measured tracer (Nb, Ta, or Al) concentration in the sample, and $(Ti/Tracer)_{background}$ is the natural background Ti to tracer elemental concentration ratio. The average natural background elemental concentration ratios of Ti to Nb, and Ti to Al for three reference soil samples within the sampling area were 322 ± 75 (Table S2), and 0.049 ± 0.003 (Smith

et al., 2013), which is in close proximity of the average crustal elemental concentration ratios (320 and 0.047, respectively) (Rudnick and Gao, 2003). The average crustal Ti to Ta was used as the natural background elemental ratio of Ti to Ta because Ta concentration in the reference soil samples was not reported (Smith et al., 2013).

2.6. Transmission electron microscope

Select < 450 nm extracted suspensions were analyzed by TEM for visual evidence of existence of engineered TiO_2 particles by looking at the distinct morphological properties of engineered compared to natural particles. Samples were prepared for TEM analysis by drop deposition on a carbon coated TEM grid (Prasad et al., 2015). The surface of the TEM grids was functionalized with a positively charged poly-L-lysine polymer (Sigma Aldrich, USA) to enhance particle retention on the grids. For TEM grid surface functionalization, the TEM grids were covered with a droplet of 0.1 % poly-L-lysine for 15 min followed by rinsing three consecutive times in ultrahigh purity water to remove excess poly-L-lysine. After functionalization, 20 µl of the fraction was pipetted on the 300 mesh Cu TEM grid (Ted Pella, Pelco). After 20 min, the excess water was removed using a filter paper. Then the grid was rinsed with UPW three times to prevent particle aggregation (Buffleben et al., 2002). After the rinse, the TEM grid was transferred to a covered grid holder for further drying.

Samples were analyzed on a LaB_6 JEOL 2100 Transmission Electron Microscope, operated at 200 keV and equipped with a JEOL EX-230 Silicon Drift Detector (SDD) with a 60 mm^2 window of acquisition for Energy Dispersive Spectra (EDS) of elements (JEOL USA Inc.).

3. Results and discussion

3.1. Total, natural and engineered Ti concentrations in bulk soils and sediments

The total concentrations of Ti in all samples varied from 1300 to 2500 mg kg^{-1} (Fig. 2). For the samples collected in Los Angeles County, the total Ti concentrations in LA1 and LA2 were not significantly different, but they were higher than those measured in LA3. The samples from LA4 and LA5 have similarly high Ti concentrations, which are similar to Ti concentrations in LA1 and LA2. For the four samples collected in Orange County, OC1 has a significantly higher Ti concentration than the other three samples. The OC4 (sediment from the stormwater retention basin) has the lowest total Ti content among all nine samples: 1312 ± 76 mg kg^{-1}. The Ti concentration increased following the order OC4 < OC2 ~ OC3 ~ LA3 ~ < LA5 ~ LA4 ~ OC1 ~ LA2 < LA1. The differences in the total Ti concentration could be attributed to differences in the natural and/or anthropogenic Ti concentrations. The differences in natural Ti concentrations among the different samples could be attributed to differences in soil origin and weathering conditions. The differences in anthropogenic Ti concentrations can be affected by several factors including drainage area, impervious cover, SGI age, and proximity to anthropogenic Ti sources.

The elemental ratios of Ti to Nb, Ti to Al, and Ti to Ta were used to identify and quantify anthropogenic Ti concentrations in SGI soils. The elemental ratio of Ti to Nb for all SGI soil samples was higher than the natural background Ti to Nb elemental ratio (Fig. 3a). The highest ratio was 598 ± 90 for LA5, followed by LA4, LA1, OC2, OC1, LA2, OC3, and LA3 (429 ± 5). The elemental ratio of Ti to Ta was higher than the natural background elemental ratio in all samples except OC4, and followed the same order as that for Ti to Nb (Fig. 3b), with strong correlation between the two elemental ratios (Fig. 3d). This is because Nb and Ta display strongly coherent geochemical behavior (Barth et al., 2000), and are naturally concentrated in natural TiO_2 minerals, which have been shown to be the dominant carrier phase (> 90-95 % of whole rock content) for Nb and Ta (José and Wyllie, 1983; Nakashima and Imaoka, 1998). The elemental ratio of Ti to Al was higher than the natural background Ti to Al elemental ratio for all samples, except OC2, OC3, and LA3 (Fig. 3c). This might be attributed to sample co-contamination with anthropogenic Ti- and Al-rich particles. Al_2O_3 is widely used in the urban environment, which is likely to result in its release to the urban environment (Hudson et al., 2002). Additionally, aluminum hydroxides are used for coating TiO_2 pigments and ENPs. All TiO_2 ENPs, except TiO_2 used as a food additive, contains 1%–15% artificial coatings by weight, most commonly oxyhydrates and oxides of silicon and aluminum (Hong et al., 2017). On the other hand, Nb and Ta are rarely used in the urban environment (Mackay and Simandl, 2014). Nb and Ta are mainly used in corrosion prevention, micro-electronics, specialty alloys, and high-strength low-alloy steel, which are likely to result in minimal release of these elements into the urban environment (Mackay and Simandl, 2014). Thus, Nb and Ta, are more suitable to differentiate and quantify the concentrations of natural from anthropogenic Ti in this study. Overall, the higher elemental ratios of Ti to Nb, Ti to Ta, and Ti to Al compared to the corresponding natural background elemental ratios suggest that all samples were contaminated with anthropogenic Ti-rich particles.

The elemental ratio of Ce to La in all samples was very close to the natural background Ce to La elemental ratio (Fig. S2a), suggesting that these soils and sediments were not or were slightly contaminated with anthropogenic Ce-rich particles. Similarly, the elemental ratio of Zr to Hf in all samples was not significantly different from the natural background Zr to Hf elemental ratio (Fig. S2b), suggesting that these samples were not contaminated with anthropogenic Zr-rich particles. These results also provide further evidence of the accuracy of the digestion and analysis protocols.

The concentration of TiO_2 engineered particles estimated based on Ti to Nb elemental ratio varied between 555 ± 13 mg kg^{-1} and 1792 ± 203 mg kg^{-1} (Fig. 4a). All SGI received parking lot runoff and are located in urban, industrial, or commercial areas with various potential sources of TiO_2 engineered (nano)-particles (Table 1). In Orange County, the concentration of TiO_2 engineered particles decreased following the order OC1 > OC2 > OC3 > OC4. The high concentration of TiO_2 engineered particles in OC1 is likely because it is the only site that receives runoff from parking lots and is surrounded by several industrial facilities, including coating facilities, welding shops, compressed natural gas fueling stations, and auto parts manufacturers. As a result, increased emission and atmospheric deposition of TiO_2 engineered (nano)-particles may result in high concentrations of TiO_2 engineered (nano)-particles in stormwater. On the other hand, OC3 is a very recent facility (put into service in 2016), which may result in a low concentration of TiO_2 engineered (nano)-particles deposited in the top layer of the bioretention system. OC4 (*e.g.,* sediment from the retention

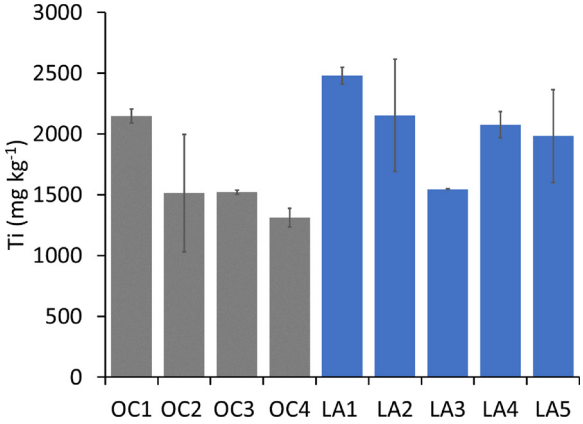

Fig. 2. Total Ti concentration in soils collected from 9 sites measured by inductively coupled plasma-mass spectrometer following digestion. Samples from different areas are presented in different colors; Orange County in gray, and Los Angeles in blue.

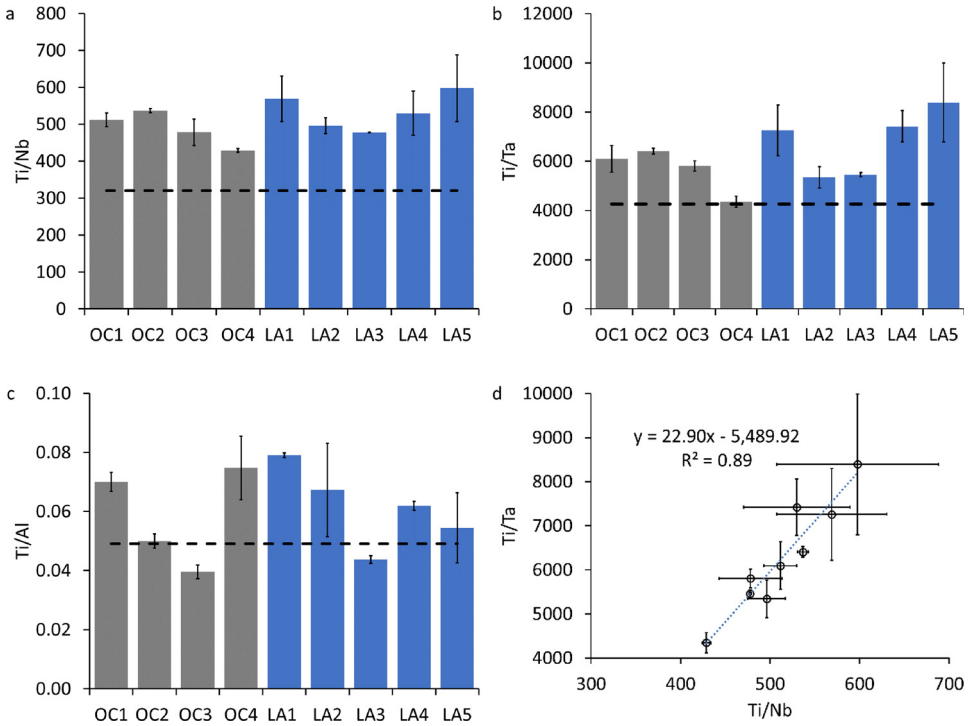

Fig. 3. Elemental ratios of (a) Ti/Nb, (b) Ti/Ta, (c) Ti/Al, and (d) correlation between Ti/Nb and Ti/Ta. The dashed lines represent the natural background value of the elemental ratios. Samples from different areas are presented in different colors; Orange County in gray, and Los Angeles in blue.

pond) had the lowest TiO_2 engineered particle concentration relative to all other SGI. Such low concentration in the sediment can be attributed to two possible reasons. The first is that the low concentration of TiO_2 engineered particles in the runoff is coming into the retention pond due to particle removal by the upstream stormwater control measures. The second is the limited sedimentation of TiO_2 (nano)-particles given the hydraulic retention time of the retention pond. Particles in retention ponds are removed from the water column by gravitational sedimentation, and thus, only large particle aggregates are preferentially removed. On the other hand, all other SGI systems remove particles from the stormwater *via* sedimentation, filtration, and adsorption. In LA County, the concentration of TiO_2 engineered particles increased following the order LA3 < LA2 < LA4 ~ LA5 < LA1. The high concentration of TiO_2 engineered (nano)-particle in LA5 can be attributed to its location near an urban/industrial site and it is proximity to a freeway (dual carriageway of 5 lanes each Golden State Freeway, LA, CA) which is a major source of TiO_2 release from white road marking (Wang et al., 2019) (Table 1). High TiO_2 engineered (nano)-particle concentration was measured in LA4 despite its location in residential/urban area from which low TiO_2 emissions might be expected and its distance from major traffic sources which are expected to be a major source of TiO_2 release (Wang et al., 2019). However, the high TiO_2 engineered (nano)-particle concentration measured in LA4 might be attributed to its large drainage area compared to all other SGI in LA County (Table 1). The lowest TiO_2 engineered (nano)-particle concentration was measured in LA3, which infiltrate runoff from a parking lot in an urban area. The higher TiO_2 engineered (nano)-particle concentration in LA1 relative to that measured in LA2 was surprising because LA1 sample site is not a SGI site. The LA1 sample was collected from a spot that is approximately 10 m away from the LA2 sampling location. While LA1 was not within the biofilters, the sampling spot was not protected from exposure to runoff.

The concentrations of TiO_2 engineered particles estimated based on Ti to Ta elemental ratio were similar to those estimated based on Ti to Nb elemental ratio in all locations except in OC4, LA2 and LA3 (Fig. 4a), and exhibited strong correlation (Fig. 4b). These differences might be due to differences in the natural background Ti to Ta elemental ratio in the SGI soils relative to the average crustal Ti to Ta elemental ratio or due to small differences in the natural elemental ratios between the different sites, and these possible differences will be further investigated in future studies.

The occurrence of TiO_2 engineered (nano)-particles in high concentrations in SGI systems is in good agreement with the extensive use of TiO_2 engineered (nano)-particles in the urban environment as ENPs

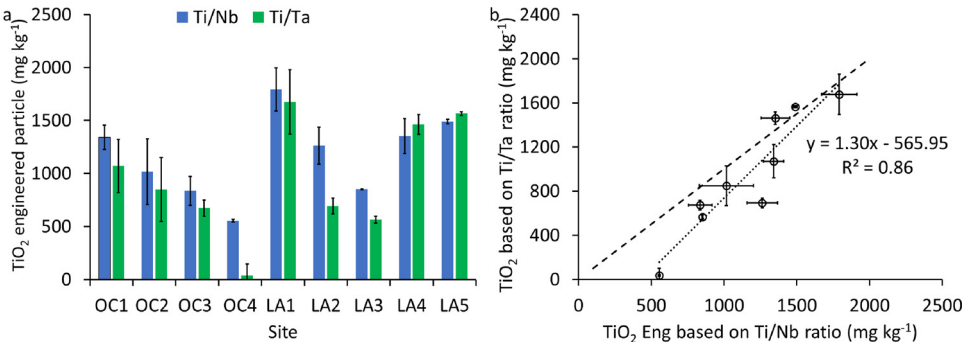

Fig. 4. (a) Concentration of TiO_2 engineered particles calculated based on Equation 1 & 2 and using Nb and Ta as a tracers of natural TiO_2 particles. (b) Correlation between TiO_2 concentrations calculated based on Ti/Nb and Ti/Ta elemental ratios. The dotted and dashed lines in (b) display the optimal (least squares) and the ideal (TiO_2 based on Ti/Nb = TiO_2 based on Ti/Ta) correlations.

in self-cleaning surfaces and as pigment in paint and coatings (Chemours, 2018; Shandilya et al., 2015), which have been shown to be released by wear and weathering (Gohler et al., 2010; Koponen et al., 2011; Nored et al., 2018; Shandilya et al., 2014a, b); and the occurrence of TiO_2 engineered (nano)-particles in road dust, atmospheric particulate matter (Lee et al., 2016; Wilczynska-Michalik et al., 2014), and urban runoff (Wang et al., 2019). SGI systems are designed to capture contaminants in stormwater before release to surface waters, and thus are a major compartment for accumulation of TiO_2 engineered (nano)-particles after release from urban settings.

3.2. Particle extraction

3.2.1. Effect of extractant on elemental concentrations and ratios

The total Ti concentration in the bulk LA4 soil was 2076 ± 109 mg kg^{-1}. For both extractants (UPW and $Na_4P_2O_7$), the measured Ti concentration decreased with the decrease in particle size cut-off (Fig. 5a). The Ti concentration in the $Na_4P_2O_7$-extracted particles were 99 ± 2 mg kg^{-1} (*ca.* 4.8 % of the total bulk soil Ti), 56 ± 2 mg kg^{-1} (*ca.* 2.7 % of the total bulk soil Ti), and 1.6 mg kg^{-1} (*ca.* 0.08 % of the total bulk soil Ti) for the < 1000 nm, < 450 nm, and < 100 nm size fractions. The Ti concentrations in the UPW-extracted particles were much lower than those in the $Na_4P_2O_7$-extracted particles and were 0.32 ± 0.03 mg kg^{-1}, 0.22 ± 0.03 mg kg^{-1}, and 0.15 ± 0.01 mg kg^{-1} for the < 1000 nm, < 450 nm, and < 100 nm size fractions, respectively, representing less than 0.02 % of the total Ti concentration in the bulk soil for all size fractions. Nb and Ta followed the same trend as Ti (Fig. S3).

The higher elemental concentrations in $Na_4P_2O_7$-extracted suspensions relative to the UPW-extracted suspensions is in good agreement with the previous studies demonstrating the extraction of higher concentrations of natural and engineered particles by $Na_4P_2O_7$ than by UPW (Loosli et al., 2018a, b). UPW together with sonication is not sufficient to break heteroaggregates. Pyrophosphate, a metal chelator, can reduce free multivalent ion concentration in the extracted suspensions, which enhances particle disaggregation by enhancing particle surface charge and reducing particle aggregation *via* bridging mechanism (Philippe and Schaumann, 2014) and/or multivalent cation specific adsorption (Jolivet, 2000).

The elemental ratio of Ti to Nb for the bulk LA4 soil was 530 ± 60 (Fig. 5b). For UPW-extracted particles, the elemental ratio of Ti to Nb decreased with the decrease in particle size and was 523 ± 19, 439 ± 33, and 345 ± 31 for the < 1000, < 450, and < 100 nm fractions, respectively, (Fig. 5b), indicating the extraction of TiO_2 engineered particles as aggregates dominantly in the < 1000 and < 450 nm size fractions. The elemental ratio of Ti to Nb in the < 100 nm fraction was very close to the natural background elemental ratio indicating that the majority of the extracted-TiO_2 nanoparticles in this size fraction are natural particles. This is likely due to inefficiency of UPW extraction to disaggregate ENPs from soil heteroaggregates into their primary particles. For $Na_4P_2O_7$, the elemental ratio of Ti to Nb ratio increased in the extracted particle fractions following the order < 1000 nm (675 ± 12), < 450 nm (722 ± 14), < 100 nm (880 ± 2). This result indicates the extraction of TiO_2 engineered (nano)-particles in all size fractions, which can be attributed to the improved disaggregation of heteroaggregates in the presence of pyrophosphate and the release of TiO_2 ENPs from soil heteroaggregates as primary particles.

The concentrations of natural and engineered Ti decreased with the decrease in particle size for both UPW- and $Na_4P_2O_7$-extracted particles (Fig. 5c and d). Nonetheless, the concentrations of natural and engineered Ti were higher in the $Na_4P_2O_7$-extracted particles relative to the UPW-extracted particles. The concentration of natural Ti in the UPW-extracted particles varied between 0.14 and 0.19 mg kg^{-1}, whereas the concentration of engineered Ti in UPW-extracted particles varied between 0.17 and 0.12 mg kg^{-1}. In contrast, the concentration of natural Ti in the $Na_4P_2O_7$-extracted particles varied between 5.8 and 47.1 mg kg^{-1}, and the concentration of engineered Ti in the $Na_4P_2O_7$-extracted particles varied between 15.8 and 57.3 mg kg^{-1}. Thus, $Na_4P_2O_7$ is more efficient in extracting natural and engineered particles and in disaggregating heteroaggregates to smaller sizes, which facilitate their analysis using other analytical techniques such as AF4-ICP-MS (**see** section 3.**5**) (Loosli et al., 2018b; Yi et al., 2019).

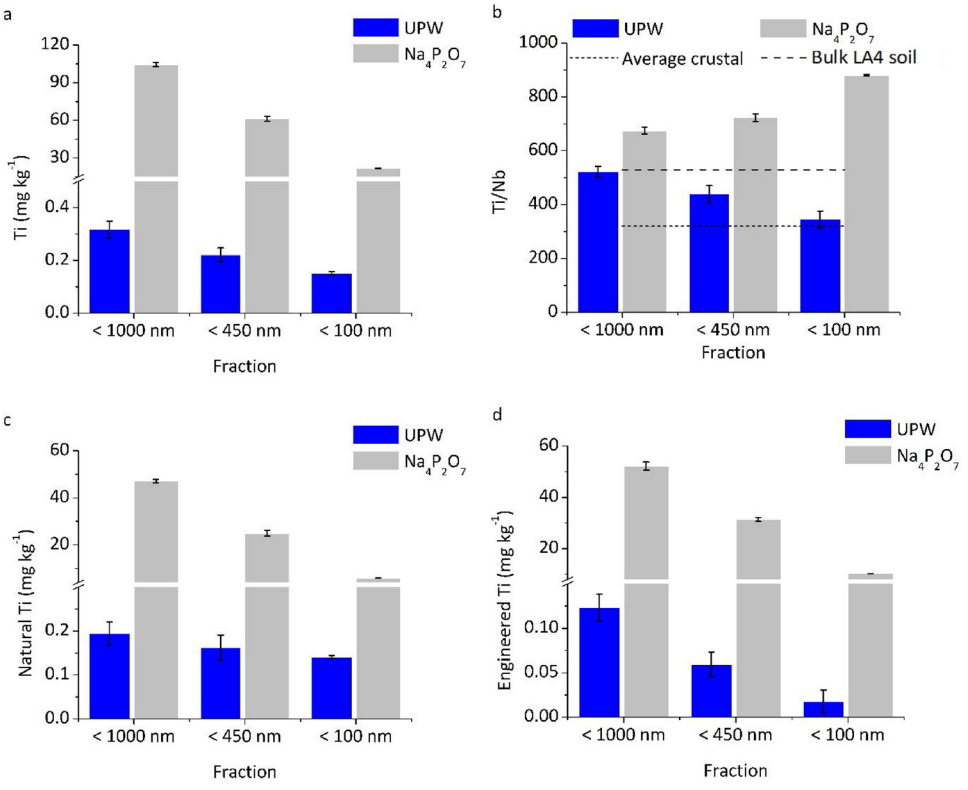

Fig. 5. Effect of extractant (ultrapure water, UPW, and sodium pyrophosphate, $Na_4P_2O_7$) on the elemental ratios and natural and engineered TiO_2 concentration in the different size fractions extracted from LA4. Soil mass to extractant ratio was 1:10. Total, natural and engineered Ti concentrations in LA4 soil were 2076 ± 109 mg kg^{-1}, 1265.7 ± 208 mg kg^{-1}, and 811 ± 99 mg kg^{-1}. The elemental ratio of Ti to Nb in the bulk LA4 was 530 ± 60.

3.2.2. Effect of soil to extractant ratios on elemental concentrations and ratios

For a given soil mass to extractant volume ratio, the concentration of the extracted Ti decreased with the decrease in particle size (Fig. 6a), indicating that most Ti-rich particles were extracted dominantly in the form of aggregates or as large particles. For a given size fraction, the concentration of the extracted Ti increased with the decrease in soil mass to extractant volume ratio (Fig. 6a). This is likely due to the increased particle dispersion with the increase in the extractant volume to soil mass ratio. For the same extractant volume, lower soil mass results in more thorough interactions between particles and $Na_4P_2O_7$, leading to better disaggregation of soil aggregates. The maximum extracted Ti concentration in the < 1000 nm, < 450 nm, and < 100 nm fractions represented 13.6 %, 9.2 %, and 3.0 % of the total Ti in the bulk soil. This is in good agreement with previous studies that demonstrated the extraction of a small fraction (*ca.* < 20 %) of Ti in a model TiO_2-clay mixture in synthetic soft water, and from natural soils (Loosli et al., 2018a).

For soil to extractant ratios of 1:10 and 1:100, the elemental ratio of Ti to Nb increased with the decrease in particle size, indicating the extraction of larger amounts of TiO_2 engineered (nano)-particles or smaller amounts of natural Ti-rich particles. For each size fraction, the elemental ratio of Ti to Nb decreased with the decrease in the soil to extractant ratio (Fig. 6b), indicating the extraction of higher concentrations of natural Ti relative to engineered Ti with the decrease in particle size. The changes in the elemental ratio of Ti to Nb as a function of the soil to extractant ratios provide further evidence on the contamination of SGI soils with TiO_2 engineered particles. This is because, in noncontaminated soils, the elemental ratio of Ti to Nb did not change as a function of extractant type, concentration, or pH due to the strong association between Ti and Nb in the same mineral phases (Loosli et al., 2019; Yi et al., 2019). Natural TiO_2 minerals have been shown to be the dominant carrier phase (> 90-95 % of whole rock content) for Nb (José and Wyllie, 1983; Nakashima and Imaoka, 1998). Although particle extraction might enhance the differences in the elemental ratio of Ti to Nb relative to the natural background ratio in the extracted particle suspension relative to that in the bulk soil, $Na_4P_2O_7$ extracts only a small fraction of the total TiO_2 engineered (nano)-particles in soil under the experimental conditions used in this study. The enhancement in the elemental ratio following extraction is due to the high concentrations of TiO_2 engineered (nano)-particles in these soils. The effect of extractant on the elemental ratio depends on the concentrations of natural Ti-rich particle and TiO_2 engineered (nano)-particles in a given sample. Extraction of higher concentrations of natural particles than engineered particles could result in a decrease in the elemental ratios of Ti to Nb.

The concentration of extracted natural Ti decreased with a decrease in the extracted particle size (Fig. 6c). For a given size fraction, the concentration of extracted natural Ti increased with a decrease in soil to extractant ratio, indicating the improved natural Ti extraction with the reduction in soil to extractant ratio. The maximum extracted natural Ti concentrations (*e.g.,* for the soil to extractant ratio of 1:10) in the < 1000 nm, < 450 nm, and < 100 nm size fractions represented approximately 17.7 %, 12.7 %, and 4.8 % of the natural Ti concentration in the bulk soil.

For a give size fraction, the concentration of the extracted engineered Ti increased with the decrease in soil to extractant ratio, except for the 100 nm size fraction. The concentration of the extracted engineered Ti in the < 100 nm size fraction (*e.g.,* ENPs; Fig. 6d) was constant at ~ 26 mg kg^{-1} for the soil to extractant ratio of 1:100 and 1:1000, indicating that this is the maximum concentration of extractable TiO_2 ENPs under the experimental conditions used in this study, which represents approximately 3.1 % of the engineered Ti concentration in bulk soil. The maximum extracted engineered Ti concentrations (*e.g.,* soil to extractant ratio of 1:1000) in the < 1000 nm, < 450 nm, and < 100 nm size fractions, respectively, represented approximately 19.7 %, 12.4 %, and 3.1 % of the engineered Ti concentration in the bulk soil. These results indicate that the majority of TiO_2 engineered particles occurred either as pigment sized particles, or as aggregates of ENPs, or mixture of both.

3.3. Size distribution of natural and anthropogenic TiO_2

Total elemental concentrations and elemental ratios provide information on the total particle concentrations. On the other hand, centrifugation coupled with total elemental concentration and elemental ratios provide information on the particle concentration within

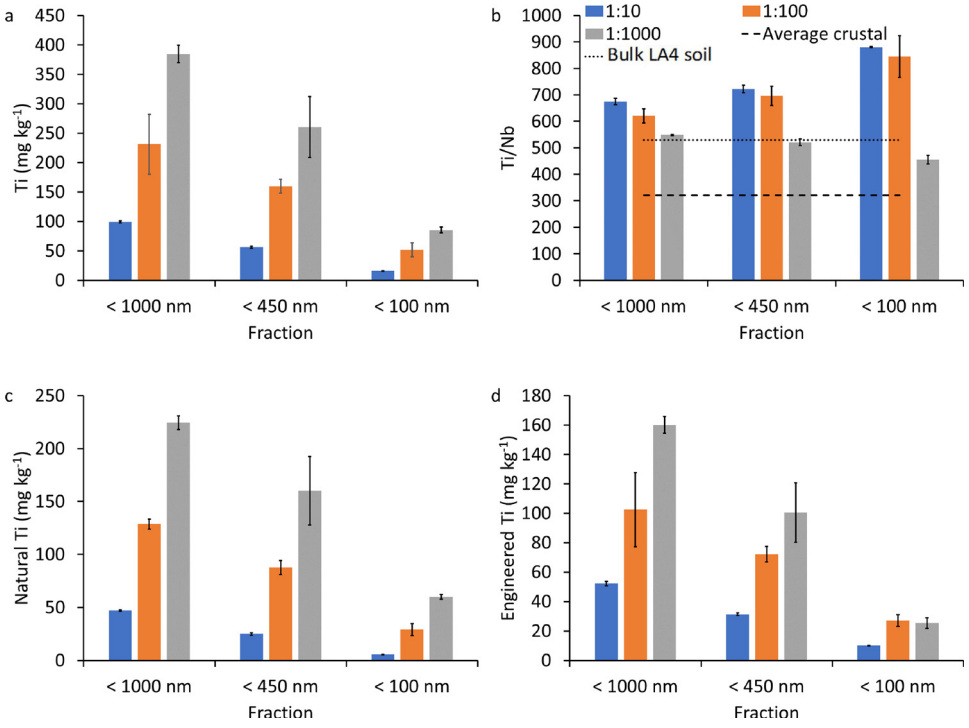

Fig. 6. Effect of soil to extractant mass ratio on the recovered natural and engineered Ti concentrations in the different size fractions (< 1000 nm, < 450 nm, and < 100 nm) extracted from LA4: (a) total Ti concentration, (b) elemental ratio of Ti to Nb, (c) natural Ti concentration and (d) engineered Ti concentration. Total, natural and engineered Ti concentrations in the bulk LA4 soil were 2076 ± 109 mg kg^{-1}, 1265.7 ± 208 mg kg^{-1}, and 811 ± 99 mg kg^{-1}. The elemental ratio of Ti to Nb in the bulk LA4 soil was 530 ± 60.

an arbitrary size window, but do not allow the determination of nanoparticle size distribution. The Ti and Nb particle size distribution of the < 450 nm $Na_4P_2O_7$ extracted particles (for the soil to extractant ratio of 1:10, LA4) was analyzed by AF4-ICP-MS (Fig. 7a) and shows that both elements co-elute at the same hydrodynamic diameters. The elemental ratio Ti to Nb (Fig. 7b) increased with the increase in the particle hydrodynamic diameter from 320 at *ca.* 5 nm to 1097 at 60 nm and remained constant for larger particles, further confirming the contamination of the soil with TiO_2 engineered particles. In non-contaminated soil, the elemental ratio of Ti to Nb was constant at approximately 300 as a function of particle size (Loosli et al., 2019; Yi et al., 2019).

The concentration of engineered Ti as a function of particle size (Fig. 7c) indicates that the majority of TiO_2 engineered (nano)-particles in the < 450 nm extracted suspensions (61 %) were smaller than 100 nm. These results further confirm that the TiO_2 engineered particles in the bulk soils are a mixture of ENPs and pigments or aggregates of ENPs. The higher proportion (*e.g.* 61 %) of engineered Ti in the < 100 nm size fraction estimated from AF4-ICP-MS compared to those estimated from filtration (*e.g.* 25 %) might be attributed to preferential retention of larger particles in the AF4 channel due to particle-membrane interactions evidenced by the tailing in the AF4 fractogram (Fig. 7c) and the elution of a peak at the end of the run when the AF4 field was reduced to zero (data not shown here). It is worth noting here that the TiO_2 size distribution is that of the extracted particles and does not necessarily represent the actual size of all TiO_2 particles in the soil due to the low TiO_2 extraction efficiency as discussed above. Thus, this study demonstrated, for the first time, that AF4-ICP-MS can be implemented for the detection and quantification of TiO_2 engineered (nano)-particles in natural soils and sediments.

The occurrence of TiO_2 engineered particles in a selected set of samples (*e.g.,* LA1 and LA4 soils; < 450 nm) was further confirmed by TEM-EDX. Fig. 8a show two spherical particles of 200 nm diameter that were identified in the LA1 extracted fraction. The elemental analysis demonstrated that these particles were composed of Ti and O (Fig. 8c). Figs. 8b and S4 show an heteoaggregate of TiO_2 particles and to Al-, Fe-, Cu- and Zn-rich particles that was observed in LA4. These particles are similar (*e.g.,* size and shape) to those TiO_2 particles observed in sludge and in landfill leachate (Kaegi et al., 2017; Kim et al., 2012; Pradas del Real et al., 2018).

4. Conclusions and perspectives

Here, we demonstrated, for the first time, the occurrence of high concentrations (*e.g.,* 550 ± 13 − 1800 ± 200 mg kg^{-1}) of TiO_2 engineered particles (both nano and pigment sized particles) in the top layer of storm green infrastructures (SGI). The occurrence of TiO_2 engineered particles in SGI soils was supported by multiple lines of evidence including **1)** the higher elemental ratios of Ti to natural tracers (Nb Ta and Al) in SGI soils relative to corresponding natural background elemental ratios, **2)** the changes in the Ti to Nb elemental ratio as a function of extractant composition and extractant volume to soil mass ratios, **3)** the increase in the Ti to Nb elemental ratio with particle size, and **4)** morphological and chemical analysis by TEM. The elemental ratios of Ti to natural tracers (Nb, and Ta) enabled quantifying the total concentrations of TiO_2 engineered particles in contaminated soils. However, the use of the elemental ratios did not allow differentiating TiO_2 pigments from TiO_2 ENPs. Particle extraction, in particular $Na_4P_2O_7$ extraction, indicated the presence of TiO_2 ENPs in the contaminated soils, which was further confirmed by a continuous size distribution analysis using AF4-ICP-MS. However, these analyses did not allow quantifying the contribution of pigments and ENPs to the total TiO_2 engineered (nano)-particles content, because it was not possible to fully extract all TiO_2 particles neither to fully disaggregate TiO_2-natural particle heteroaggregates. Such quantification will require developing approaches to fully disaggregate TiO_2 ENPs and pigments from heteroaggregates in natural environment samples.

The high concentrations (*e.g.,* 550 ± 13 − 1800 ± 200 mg kg^{-1}) of TiO_2 engineered particles in the top soil layer of SGI indicate the retention of these particles in SGI from wet- and dry- weather runoff containing high concentrations of TiO_2 engineered particles. However, the retention efficiency and downward migration of ENPs in SGI

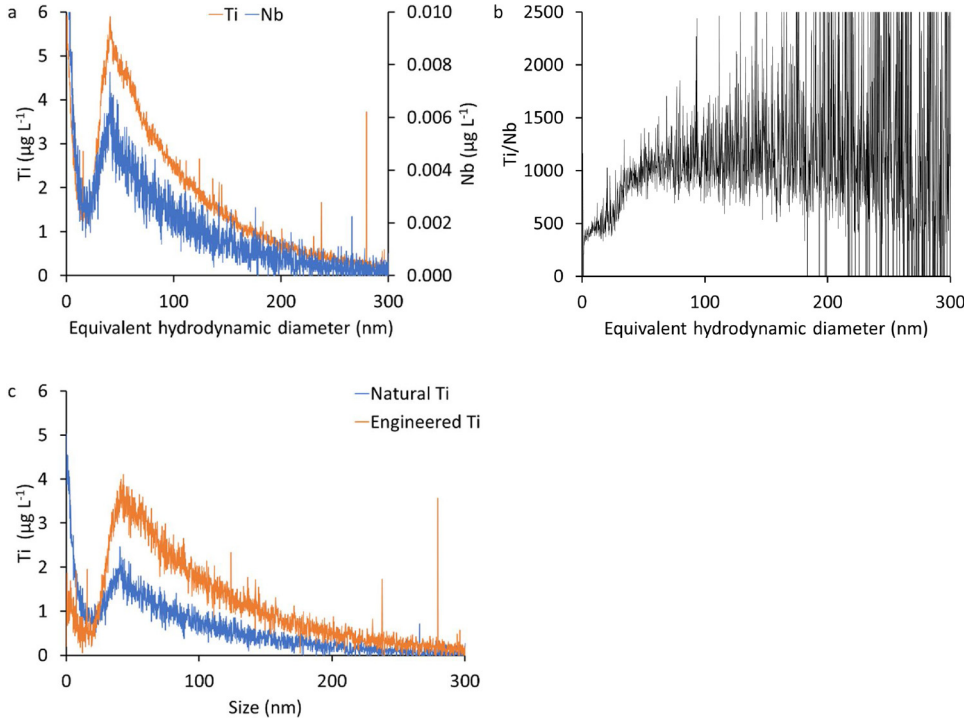

Fig. 7. Size distribution of the < 450 nm $Na_4P_2O_7$ extracted particles from LA4 soil by AF4-ICP-MS: **(a)** Ti and Nb particle size distribution, (b) elemental ratio of Ti to Nb, and (c) estimated natural and engineered TiO_2 size distributions. The soil:extractant ratio was 1:10 and the sample injection volume was 50 µL.

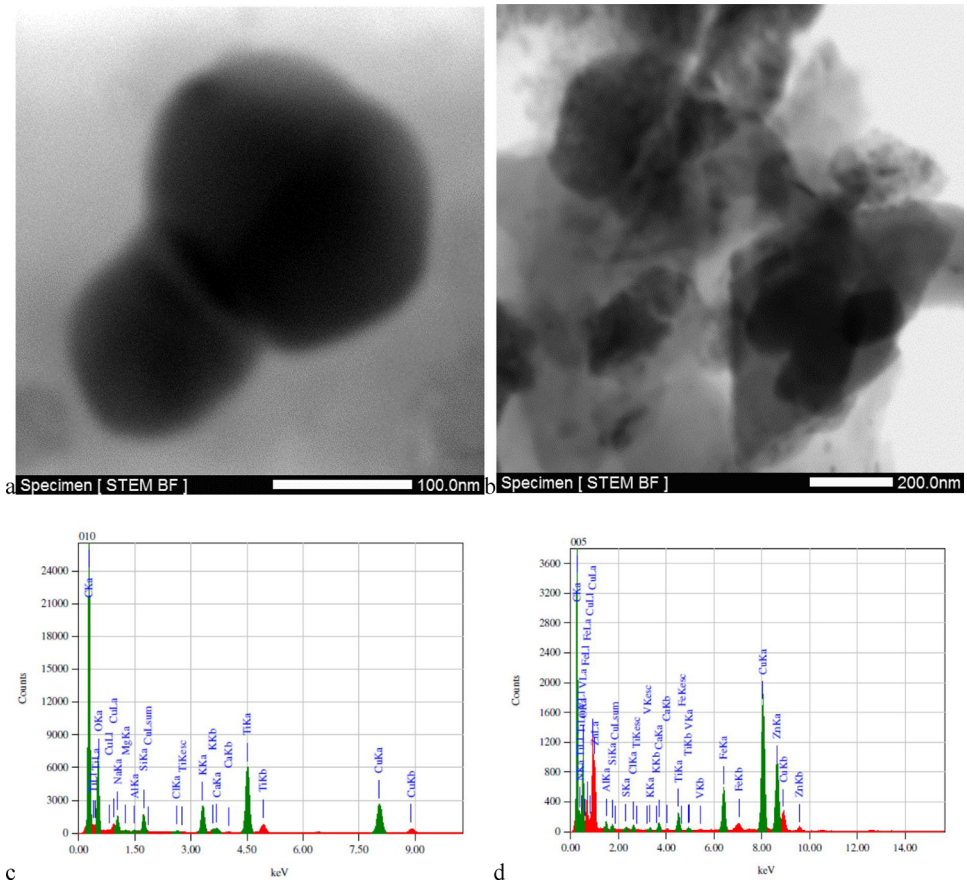

Fig. 8. Morphological and elemental composition of Ti-containing particles in the < 450 nm $Na_4P_2O_7$ extracted particles from: (a and c) LA1 soil, and (b and d) LA4 soil.

remains unknown and require further investigations using controlled laboratory experiment. The retention of TiO_2 engineered particle in SGI soil minimizes their release to surface waters and to marine waters, and thus reduces exposure of sensitive species, such as coral reefs, to TiO_2 engineered particles (Jovanovic and Guzman, 2014). However, in areas where stormwater flows directly into surface and marine waters, such organisms will be exposed to TiO_2 engineered (nano)-particles. Additionally, some TiO_2 engineered (nano)-particles pass/travel through the SGI and get released to surface waters.

These findings invite further studies aimed at comprehensive evaluation of TiO_2 engineered (nano)-particle environmental exposure, fate modeling, and ecotoxicity in the urban environment. Specifically, studies are needed that focus on understanding the factors affecting the release, fate of engineered (nano)-particles in urban runoff, retention of TiO_2 engineered particles in different SGI, the migration, distribution, and biological impacts of engineered (nano)-particles in SGI, and the best procedures for disposal of any soil media used in SGI.

Author contributions section

Dr. Baalousha conceived the overall idea of the study. Drs. Baalousha, Mohanty, Afrooz, and Aich discussed the overall strategy of the study and designed the sampling strategy. Mr. Valenca collected the SGI soil samples. Mr. Nabi and Dr. Wang performed all chemical analysis. Dr. Cantando performed transmission electron microscopy analysis. All authors contributed to writing, proof reading, and revision of the manuscript.

Declaration of Competing Interest

The authors declare that there are no conflicts of interest.

Acknowledgments

This work was supported by US National Science Foundation CAREER1553909grant to Dr. Mohammed Baalousha, Swiss National Science Foundation postdoctoral mobility funding (P2GEP2_165046) to Dr. Frédéric Loosli. This work was supported by the Virginia Tech National Center for Earth and Environmental Nanotechnology Infrastructure (NanoEarth, a member of the National Nanotechnology Coordinated Infrastructure NNCI, supported by NSF ECCS 1542100). We acknowledge Orange County Public Works (Frank Cheng) and Los Angeles County Flood Control District (Jian Peng) for their support regarding identification of candidate SGI and soil sample collections from those sites.

Appendix A. Supplementary data

Supplementary material related to this article can be found, in the online version, at doi:https://doi.org/10.1016/j.jhazmat.2020.122335.

References

Ahiablame, L.M., Engel, B.A., Chaubey, I., 2012. Effectiveness of low impact development practices: literature review and suggestions for future research. Water Air Soil Pollut. 223, 4253–4273.

ASTM, 2015. ASTM D7942-15: Standard Specification for Thermoplastic Pavement Markings in Non Snow Plow Areas. ASTM.

Baalousha, M., Yang, Y., Vance, M.E., Colman, B.P., McNeal, S., Xu, J., Blaszczak, J., Steele, M., Bernhardt, E., Hochella, J.R.M.F., 2016. Outdoor urban nanomaterials:

The emergence of a new, integrated, and critical field of study. Sci. Total Environ. 557–558, 740–753.
Barth, M.G., McDonough, W.F., Rudnick, R.L., 2000. Tracking the budget of Nb and Ta in the continental crust. Chem. Geol. 165, 197–213.
Birch, G.F., Fazeli, M.S., Matthai, C., 2005. Efficiency of an infiltration basin in removing contaminants from urban stormwater. Environ. Monit. Assess. 101, 23–38.
Buffle, J., Wilkinson, K.J., Stoll, S., Filella, M., Zhang, J., 1998. A generalized description of aquatic colloidal interactions: the three-colloidal component approach. Environ. Sci. Technol. 32, 2887–2899.
Buffleben, M.S., Zayeed, K., Kimbrough, D., Stenstrom, M.K., Suffet, I.H., 2002. Evaluation of urban non-point source runoff of hazardous metals entering Santa Monica Bay, California. Water Sci. Technol. 45, 263–268.
Chemours, 2018. Titanium Dioxide For Coating.
Coatingsworld, 2019. U.S. Demand for Paint & Coatings to Reach 1.4 Billion Gallons in 2019.
Fedotov, P.S., Vanifatova, N.G., Shkinev, V.M., Spivakov, B.Y., 2011. Fractionation and characterization of nano-and microparticles in liquid media. Anal. Bioanal. Chem. 400, 1787–1804.
Gnecco, I., Berretta, C., Lanza, L.G., La Barbera, P., 2005. Storm water pollution in the urban environment of Genoa, Italy. Atmos. Res. 77, 60–73.
Gohler, D., Stintz, M., Hillemann, L., Vorbau, M., 2010. Characterization of nanoparticle release from surface coatings by the simulation of a sanding process. Annal. Occup. Hyg. 54, 615–624.
Golanski, L., Guiot, A., Pras, M., Malarde, M., Tardif, F., 2012. Release-ability of nano fillers from different nanomaterials (toward the acceptability of nanoproduct). J. Nanopart. Res. 14, 962.
Gondikas, A.P., von der Kammer, F., Reed, R.B., Wagner, S., Ranville, J.F., Hofmann, T., 2014. Release of TiO2 nanoparticles from sunscreens into surface waters: a one-year survey at the Old Danube recreational lake. Environ. Sci. Technol. 48, 5415–5422.
Gondikas, A., von der Kammer, F., Kaegi, R., Borovinskaya, O., Neubauer, E., Navratilova, J., Praetorius, A., Cornelis, G., Hofmann, T., 2018. Where is the nano? Analytical approaches for the detection and quantification of TiO2 engineered nanoparticles in surface waters. Environ. Sci. Nano 5, 313–326.
Grand View Research, 2018. https://www.grandviewresearch.com/industry-analysis/traffic-road-marking-coatings-market/request.
Grebel, J.E., Mohanty, S.K., Torkelson, A.A., Boehm, A.B., Higgins, C.P., Maxwell, R.M., Nelson, K.L., Sedlak, D.L., 2013. Engineered infiltration systems for urban stormwater reclamation. Environ. Eng. Sci. 30, 437–454.
He, W., Wallinder, I.O., Leygraf, C., 2001. A laboratory study of copper and zinc runoff during first flush and steady-state conditions. Corros. Sci. 43, 127–146.
Hong, F., Yu, X., Wu, N., Zhang, Y.Q., 2017. Progress of in vivo studies on the systemic toxicities induced by titanium dioxide nanoparticles. Toxicol. Res. 6, 115–133.
Hudson, L.K., Misra, C., Perrotta, A.J., Wefers, K., Williams, F.S., 2002. Aluminum Oxide Ullmann's Encyclopedia of Industrial Chemistry. Wiley-VCH, Weinheim.
Huynh, K.A., Siska, E., Heithmar, E., Tadjiki, S., Pergantis, S.A., 2016. Detection and quantification of silver nanoparticles at environmentally relevant concentrations using asymmetric flow field-flow fractionation online with single particle inductively coupled plasma mass spectrometry. Anal. Chem. 88, 4909–4916.
Jolivet, J.P., 2000. Metal Oxide Chemistry and Synthesis. From Solution to Solid State. Wiley, West Sussex, England.
José, C.G., Wyllie, P.J., 1983. Ilmenite (high Mg, Mn, Nb) in the carbonatites from the Jacupiranga complex, Brazil. Am. Mineral. 68, 960–971.
Jovanovic, B., Guzman, H.M., 2014. Effects of titanium dioxide (TiO2) nanoparticles on caribbean reef – building coral (Montastraea faveolata). Environ. Toxicol. Chem. 33, 1346–1353.
Kaegi, R., Englert, A., Gondikas, A., Sinnet, B., von der Kammer, F., Burkhardt, M., 2017. Release of TiO_2 (Nano) particles from construction and demolition landfills. NanoImpact 8, 73–79.
Kim, B., Murayama, M., Colman, B.P., Hochella, M.F., 2012. Characterization and environmental implications of nano-and larger TiO 2 particles in sewage sludge, and soils amended with sewage sludge. J. Environ. Monit. 14, 1128–1136.
Kondo, M.C., Sharma, R., Plante, A.F., Yang, Y., Burstyn, I., 2016. Elemental concentrations in urban green stormwater infrastructure soils. J. Environ. Qual. 45, 107–118.
Koponen, I.K., Jensen, K.A., Schneider, T., 2011. Comparison of dust released from sanding conventional and nanoparticle-doped wall and wood coatings. J. Expos. Sci. Environ. Epidemiol. 21, 408–418.
Lee, P.K., Yu, S., Chang, H.J., Cho, H.Y., Kang, M.J., Chae, B.G., 2016. Lead chromate detected as a source of atmospheric Pb and Cr (VI) pollution. Sci. Rep. 6, 36088.
Li, C., Peng, C., Chiang, P.C., Cai, Y., Wang, X., Yang, Z., 2019. Mechanisms and applications of green infrastructure practices for stormwater control: a review. J. Hydrol. 568, 626–637.
Loosli, F., Le Coustumer, P., Stoll, S., 2014. Effect of natural organic matter on the disagglomeration of manufactured TiO2 nanoparticles. Environ. Sci. Nano 1, 154–160.
Loosli, F., Le Coustumer, P., Stoll, S., 2015. Effect of electrolyte valency, alginate concentration and pH on engineered TiO_2 nanoparticle stability in aqueous solution. Sci. Tot. Environ. 535, 28–34.
Loosli, F., Berti, D., Yi, Z., Baalousha, M., 2018a. Toward a better extraction and stabilization of titanium dioxide engineered nanoparticles in model water. NanoImpact 11, 119–127.
Loosli, F., Yi, Z., Wang, J., Baalousha, M., 2018b. Dispersion and analysis of natural nanomaterials in surface waters for better characterization of their physicochemical propoerties by AF4-ICP-MS-TEM. Sci. Total Environ. 682, 663–672.
Loosli, F., Wang, J., Rothenberg, S., Bizimis, M., Winkler, C., Borovinskaya, O., Flamigni, L., Baalousha, M., 2019a. Sewage spills are a major source of engineered titanium dioxide release into the environment. Environ. Sci. Nano 6, 763–777.
Loosli, F., Yi, Z., Wang, J., Baalousha, M., 2019b. Improved extraction efficiency of natural nanomaterials in soils to facilitate their characterization using a multimethod approach. Sci. Total Environ. 677, 34–46.
Luo, Z., Wang, Z., Li, Q., Pan, Q., Yan, C., Liu, F., 2011. Spatial distribution, electron microscopy analysis of titanium and its correlation to heavy metals: occurrence and sources of titanium nanomaterials in surface sediments from Xiamen Bay, China. J. Environ. Monit. 13, 1046–1052.
Mackay, D.A.R., Simandl, G.J., 2014. Geology, market and supply chain of niobium and tantalum – a review. Miner. Deposita 49, 1025–1047.
Mahdi, K.N.M., Peters, R.J.B., Klumpp, E., Bohme, S., Ploeg, M., Ritsema, C., Geissen, V., 2017. Silver nanoparticles in soil: aqueous extraction combined with single-particle ICP-MS for detection and characterization. Environ. Nanotechnol. Monit. Manage. 7, 24–33.
Montano, M.D., Lowry, G.V., von der Kammer, F., Blue, J., Ranville, J.F., 2014. Current status and future direction for examining engineered nanoparticles in natural systems. Environ. Chem. 11, 351–366.
Nakashima, K., Imaoka, T., 1998. Niobian and zincian ilmenites in syenites from Cape Ashizuri, Southwest Japan. Mineral. Petrol. 63, 1–17.
Navratilova, J., Praetorius, A., Gondikas, A., Fabienke, W., von der Kammer, F., Hofmann, T., 2015. Detection of engineered copper nanoparticles in soil using single particle ICP-MS. Int. J. Environ. Res. Public Health 12, 15756–15768.
Nored, A.W., Chalbot, M.C., Kavouras, I.G., 2018. Characterization of paint dust aerosol generated from mechanical abrasion of TiO2-containing paints. J. Occup. Environ. Hyg. 15, 629–640.
Part, F., Zecha, G., Causon, T., Sinner, E.K., Huber-Humer, M., 2015. Current limitations and challenges in nanowaste detection, characterisation and monitoring. Waste Manage. 43, 407–420.
Philippe, A., Schaumann, G.E., 2014. Interactions of dissolved organic matter with natural and engineered inorganic colloids: a review. Environ. Sci. Technol. 48, 8946–8962.
Pradas del Real, A.E., Castillo-Michel, H., Kaegi, R., Larue, C., De Nolf, W., Reyes-Herrera, J., Tucoulou, R., Findling, N., Salas-Colera, E., Sarret, G., 2018. Searching for relevant criteria to distinguish natural vs. anthropogenic TiO_2 nanoparticles in soils. Environ. Sci. Nano 5, 2853–2863.
Praetorius, A., Gundlach-Graham, A., Goldberg, E., Fabienke, W., Navratilova, J., Gondikas, A., Kaegi, R., Gunther, D., Hofmann, T., von der Kammer, F., 2017. Single-particle multi-element fingerprinting (spMEF) using inductively-coupled plasma time-of-flight mass spectrometry (ICP-TOFMS) to identify engineered nanoparticles against the elevated natural background in soils. Environ. Sci. Nano 4, 307–314.
Prasad, A., Baalousha, M., Lead, J.R., 2015. An electron microscopy based method for the detection and quantification of nanomaterial number concentration in environmentally relevant media. Sci. Total Environ. 537, 479–486.
Regelink, I.C., Weng, L., Koopmans, G.F., van Riemsdijk, W.H., 2013. Asymmetric flow field-flow fractionation as a new approach to analyse iron-(hydr)oxide nanoparticles in soil extracts. Geoderma 202 – 203, 134–141.
Rudnick, R.L., Gao, S., 2003. Composition of the continental crust. Treat. Geochem. 3, 659.
Shandilya, N., Bihan, O.L., Bressot, C., Morgeneyer, M., 2014a. Evaluation of the particle aerosolization from n-TiO 2 photocatalytic nanocoatings under abrasion. J. Nanomater. 2014 185080-1-185080-14.
Shandilya, N., Le Bihan, O., Morgeneyer, M., 2014b. A review on the study of the generation of (nano) particles aerosols during the mechanical solicitation of materials. J. Nanomater. 2014, 5.
Shandilya, N., Le Bihan, O., Bressot, C., Morgeneyer, M., 2015. Emission of titanium dioxide nanoparticles from building materials to the environment by wear and weather. Environ. Sci. Technol. 49, 2163–2170.
Smith, D.B., Cannon, W.F., Woodruff, L.G., Solano, F., Kilburn, J.E., Fey, D.L., 2013. Geochemical and Mineralogical Data for Soils of the Conterminous United States.
Tang, Z., Wu, L., Luo, Y., Christie, P., 2009. Size fractionation and characterization of nanocolloidal particles in soils. Environ. Geochem. Health 31, 1–10.
Tong, T., Hill, A.N., Alsina, M.A., Wu, J., Shang, K.Y., Kelly, J.J., Gray, K.A., Gaillard, J.F., 2015. Spectroscopic characterization of TiO2 polymorphs in wastewater treatment and sediment samples. Environ. Sci. Technol. Lett. 2, 12–18.
von der Kammer, F., Ferguson, P.L., Holden, P.A., Masion, A., Rogers, K.R., Klaine, S.J., Koelmans, A.A., Horne, N., Unrine, J.M., 2012. Analysis of engineered nanomaterials in complex matrices (environment and biota): general considerations and conceptual case studies. Environ. Toxicol. Chem. 31, 32–49.
Wang, H., Adeleye, A.S., Huang, Y., Li, F., Keller, A.A., 2015. Heteroaggregation of nanoparticles with biocolloids and geocolloids. Adv. Colloid Interface Sci. 226 (Part A), 24–36.
Wang, J., Nabi, M., Mohanty, S.K., Afrooz, N., Cantando, E., Aich, N., Baalousha, M., 2019. Detection and quantification of TiO_2 engineered particles in urban runoff. Chemosphere 248, 126070.
Wilczynska-Michalik, W., Rzeznikiewicz, K., Pietras, B., Michalik, M., 2014. Fine and ultrafine TiO2 particles in aerosol in Krakow (Poland). Mineralogia 45, 65–77.
Yi, Z., Loosli, F., Wang, J., Berti, D., Baalousha, M., 2019. How to distinguish natural versus engineered nanomaterials: insights from the analysis of TiO2 and CeO2 in soils. Environ. Chem. Lett. 18, 215–227.